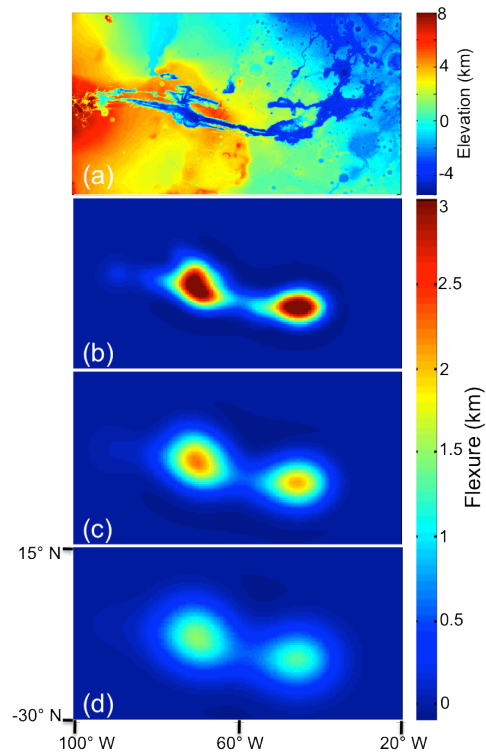


**FLEXURAL RESPONSE TO SEDIMENT EROSION AND UNLOADING AT VALLES MARINERIS, MARS.** B. J. Davis<sup>1\*</sup> and J. C. Andrews-Hanna<sup>1</sup>, <sup>1</sup>Department of Geophysics, Colorado School of Mines, Golden, CO, Brdavis@mines.edu.

**Introduction:** The origin and evolution of the Valles Marineris canyon system and its stacks of interior layered deposits (ILD) on Mars remains as one of the most debated topics in Martian tectonics. The subtle broad topographic uplift around the periphery of the canyon system conflicts with the uplifted flanks predicted by models of normal faulting [1]. This uplift is obscured in the east and west by the Thaumasia ridge and Noctis Labyrinthus, respectively, but is clear north and south of the central chasmata. The troughs and their surroundings also have a distinctive signature in the gravity field. The troughs themselves exhibit a pronounced negative gravity anomaly, indicating that the deep trough depressions are not isostatically compensated, but rather are flexurally supported as a negative load on the lithosphere. The trough flanks exhibit positive gravity anomalies.

Large-scale extensional tectonic provinces such as rift valleys on Earth form in a state of approximate vertical isostasy [2]. It is suggested that the depths of the troughs was controlled by isostatic balance with the sedimentary infill, with the troughs at one time being filled with sediment in a state of near isostasy [3]. Subsequent erosion of these sediments would have led to regional flexural uplift. Several studies have suggested that the present-day ILD's are an erosional remnant of a once more extensive set of deposits [4-6]. In this study we show that much of the topography and gravity surrounding the troughs can be explained by flexural uplift due to the removal of these sediments.

**Methods:** We used a thin-shell, elastic lithospheric loading model [7, 8] in order to determine the flexural response of the lithosphere due to the removal of a sediment load. The thickness of the erosional load (the sediments removed from the troughs) was estimated using the difference between the present-day surface topography within the troughs and 4000 m, where 4000 m was chosen as a representative elevation of the trough margins. Using this method we calculated a void space volume of  $5.02 \times 10^6 \text{ km}^3$ , consistent with previous studies [9]. The density of the sediments was assumed to be  $2500 \text{ kg/m}^3$ , representative of an equal mixture of basalt and kieserite, with a 10% porosity. The models are sensitive to the elastic thickness of the lithosphere ( $T_e$ ) which is poorly constrained. Previous lithosphere thickness estimates for Valles Marineris range from 60-200 km [10]. As a result, the flexure was modeled using a range of lithosphere thicknesses. Figures 1a-c shows the results for  $T_e = 50 \text{ km}$ , 100 km and 150 km.



**Figure 1.** Model Results. (a) MOLA topography. (b) Flexural uplift when  $T_e = 50 \text{ km}$ . (c)  $T_e = 100 \text{ km}$ . (d)  $T_e = 150 \text{ km}$ . All panels have the same north-south and east-west extents.

**Results:** The modeling predicts two main regions of flexural uplift – one in the center of the trough complex (beneath Ophir, Candor and Melas Chasmata) and one at the eastern periphery (beneath Eos and Capri Chasmata). Flexure as great as  $\sim 3.5 \text{ km}$  is predicted by the model with  $T_e = 50 \text{ km}$ , while the thicker lithospheres of 100 and 150 km predict maximum uplifts of only 2.2 and 1.5 km, respectively. The two models with thinner lithospheres also show a third, subtle region of uplift west of Melas Chasma, between Tithonium Chasma and Noctis Labyrinthus.

The predicted flexural topography can be compared with the observed topography in the vicinity of the troughs. Topographic profiles across the troughs reveal a broad dome encompassing Hebes, Ophir, Candor, and central Melas chasmata, rising to a height of 1.4 to 2.2 km above the plateau to the south (Figure 2). The topography drops further to the north, as the profiles cross the buried crustal dichotomy boundary [11]. Both the height of the dome and its lateral extent agree best with the models with lithosphere thicknesses of 100-

150 km, with the strongest agreement on the plateau south of the chasmata. The highest part of Valles Marineris is the plateau separating Candor Chasma from the Melas and Coprates Chasmata. This plateau juts directly into the region of maximum flexure predicted by the modeling, suggesting that this high topography can be explained by flexural uplift. The correlation between topography and flexural uplift extends further outward from this plateau.

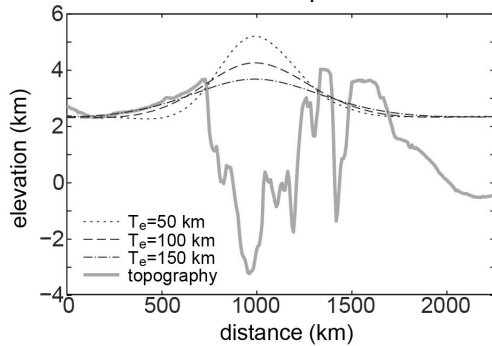


**Figure 2.** Mean profiles of MOLA topography and model uplift, from south to north averaged between 73 and 76° W

The observed flexural uplift over the second region, encompassing Eos, Capris, and Ganges chasmata, is less pronounced, and the lower flexural uplift here may be a result of a thicker lithosphere. However, because this region is located at the boundary between the main Valles Marineris complex and the outflow channels, it is unclear as to whether or not its evolution is equivalent to that of the other region. As a result, our analysis focuses on the region beneath the central chasmata, where the evolution is better understood.

The predicted free-air gravity anomalies arising from the combination of the erosion and the flexural uplift include large negative anomalies over the troughs, and a surrounding positive anomaly. Figures 3b and c show the predicted gravity anomalies that would arise from the erosion of the sediment load and the model uplift for  $T_e = 100$  and 150 km. These predicted anomalies approximately match the observed negative anomalies in Hebes, Ophir and Candor Chasmata, as well as the strong positive anomaly observed at the plateau between Candor and Melas Chasmata (Figure 3a). While the modeling does predict strong positive anomalies around the periphery of the troughs, the magnitude is  $\sim 250$  mgal less than that observed. Further, the model predicts stronger negative anomalies in Ius and weaker negative anomalies in Coprates, relative to the observed values. These discrepancies likely arise from the errors in the approximation of the eroded sediment volume. Nevertheless, these models provide strong evidence that the observed gravity anomalies in and around Valles Marineris arise

at least in part from the flexural response to sediment unloading.

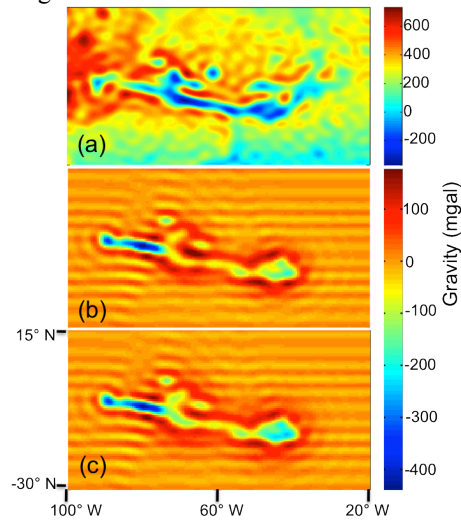


**Figure 3.** (a) Observed gravity. (b) and (c) Theoretical gravity anomaly arising from the erosion of the sediment load due and the model flexural uplift for  $T_e = 100$  km and 150 km, respectively.

**Conclusion:** There is a strong correlation between the gravity and topographic relief of the Valles Marineris region with the flexural uplift that would be expected from the unloading of sediments within the troughs. This work has implications for the tectonic evolution of Valles Marineris as this flexure induces additional extensional and compressional stresses in the region. The predicted flexural uplift would result in extensional stresses within the center of uplift identified above, and compressional stresses outside of this zone. To first order, this is consistent with structural studies of the ILD's revealing extensive tectonic modification, with the last episode being the formation of tensile joints [4]. Further work will involve calculating these stresses to understand how they interact with the regional stress field, and improving on existing crustal thickness models of the region in order to more accurately determine Moho relief.

**References:** [1] Schultz, R. A. and Lin, J. (2001) *JGR* 106 16,549-16,566. [2] Karner, G. D. et al. (2005) *Earth and Planet. Sci. Lett.* 235 577-596. [3] Andrews-Hanna, J. C. (2011) *LPSC*, abstract 2182. [4] Okubo, C. H. (2010) *Icarus* 207 210-225. [5] Roach, L. H. et al. (2010) *Icarus* 207 659-674. [6] Murchie, S. L. et al. (2009) *JGR* 114, E00D05, doi:10.1029/2009JE003343. [7] Johnson, C. L. et al. (2000) *Icarus* 144 313-328. [8] Willeman, R. J. and Turcotte, D. L. (1981) *LPSC* 12, 837-851. [9] Lucchitta, B. K. et al. (1994) *JGR* 99, 3783-3798. [10] McGovern, P. J. et al. (2004) *JGR* 109, doi:10.1029/2004JE002286. [11] Andrews-Hanna, J. C. et al. (2008) *Nature* 453 1212-1215.